Scientia Iranica (2024) 31(16), 1431–1449

Sharif University of Technology
Scientia Iranica
Transactions B: Mechanical Engineering
https://scientiairanica.sharif.edu

Contouring error prediction and optimization of stone relief for robotic milling

Fangchen Yin[a,b,*] and Hongyuan Zhang[a,b]

a. *National and Local Joint Engineering Research Center for Intelligent Manufacturing Technology of Brittle Material Products, Huaqiao University, Xiamen 361021, China.*
b. *Institute of Manufacturing Engineering, Huaqiao University, Xiamen 361021, China.*

Received 9 November 2021; received in revised form 4 July 2023; accepted 28 November 2023

KEYWORDS
Stone relief;
Mechanical arm milling;
Response surface methodology;
Contour error;
Process parameter optimization.

Abstract. Contour error is a crucial quality measure for stone relief products. Achieving the appropriate process parameters is vital due to the inherent hardness, brittleness, and natural crystal defects found in white marble. This study investigated various processing characteristics of Chinese character stone relief and primarily focused on understanding the impact of spindle speed, feed speed, milling width, and milling depth on contour error. The study optimized the process parameters by considering the contour error as the response target. Firstly, the paper outlined the machining process of stone relief using a manipulator and provided a classification basis for different machining features. Subsequently, a series of white marble milling experiments were conducted using the Box-Behnken design method of Response Surface Methodology (RSM). A multiple nonlinear regression model was established to analyze the influence of various processing characteristics on white marble contour error. Through RSM, the interaction effects of different factors on the contour error were examined. Finally, optimal milling parameters were selected and validated through experiments. The results indicated that the optimized milling process proposed in this study can reduce the contour error of the final stone relief products by 47.3% compared to traditional milling methods.

1. Introduction

In the stone industry, stone relief products are the perfect combination of stone and carving art. It has been recording the development of world civilization. As the main carrier of human culture and art inheritance, they have extremely high artistic and cultural values [1,2]. At the same time, white marble relief products are the highest added value stone products due to their clear color and fine texture. The traditional manual processing method of white marble relief products has a long cycle, low productivity and high labor costs, and the quality of the product depends entirely on the accumulation of expertise of the workers, resulting in low yield and difficulty in meeting quality requirements. Therefore, the application of the robotic arm to the white marble carving not only realizes the "machine

*. *Corresponding author. Tel.: +86 18159284929*
E-mail addresses: yfc_ral@163.com (F. Yin); 1026145201@qq.com (H. Zhang)

To cite this article:
Fangchen Yin and Hongyuan Zhang "Contouring error prediction and optimization of stone relief for robotic milling", *Scientia Iranica* (2024), **31**(16), pp. 1431–1449
https://doi.org/10.24200/sci.2023.59368.6200

substitution, flexible manufacturing", but also makes up for the shortcomings of traditional white marble Computer Numerical Control (CNC) engraving, such as the small working range, the inability to process large and super large relief products, and the insufficient processing posture. It is the future development direction of stone carving processing [3,4].

In the milling process of stone relief products using a robotic arm, the stone blanks are prone to chipping or fracture due to the weak rigidity structure of the robotic arm, the hardness and brittleness of white marble, and natural crystal defects. Therefore, it is crucial to select appropriate process parameters [5]. Accurately predicting the trend of processing quality of white marble and exploring the relative relationship between process parameters and processing quality can effectively guide the selection and adjustment of process parameters, ensuring the stability of processing quality of stone relief products, which is an effective and low-cost way to promote the large-scale application of robotic arm in the field of stone relief processing [6]. There are many features that characterize the processing quality of stone relief products, one of the most effective feature is the contour error. It is difficult to establish an accurate stone contour error model through theoretical analysis due to the non-linearity and difficult determinism between the contour error and the process parameters. With the development of intelligent technology, the construction of intelligent models has provided a new way for the establishment of predictive models in mechanical processing in recent years. The artificial intelligence model can choose the appropriate optimization scheme according to different problems, whether it is in the establishment of the prediction model of milling force, surface roughness, or machining error, the intelligent modeling method shows excellent performance [7,8].

There are many ways to construct intelligent models, the neural network method, Taguchi method and response surface method etc. are commonly used. The neural network method can highly approximate nonlinear systems and has adaptive and self-learning capabilities for complex uncertain systems [9], but it will prematurely converge to the local optimal solution of the objective function, making it difficult to find the global optimal untie. Taguchi method is simple and ingenious., it's variable types can be continuous or discrete, but the interaction between factors cannot be clearly defined by it [10]. The modeling prediction based on response surface method has been more widely used in the machining field compared with other intelligent modeling methods due to its advantages of simple modeling, less test times, and response value closer to the real results [11,12]. For the Electrical Discharge Machining (EDM) process of titanium alloys, Ghodsiyeh et al. used the response surface method to establish a prediction model between pulse turn-on, pulse preparation time, current and surface roughness, and verified the effectiveness of the prediction model [13]. Lmalghan et al. studied the changes of milling force and surface roughness in the process of milling AA6061 aluminum alloy, and compared the accuracy of the milling force and surface roughness prediction model formed respectively by particle swarm algorithm and Response Surface Method (RSM) [4]. Unune et al. studied the process of EDM diamond grinding Inconel 718 through orthogonal experiments, and established a surface roughness model by using response surface methodology, and analyzed the influence of machining parameters on surface roughness [15]. Lin et al. used the response surface method to analyze the influence of RuT400 alloy grinding parameters on the surface roughness, and obtained the significance ranking of the influencing factors [16]. Lu et al. studied the influence of spindle speed, single tooth feed, and axial grinding depth on the Vickers hardness of Inconel 718 alloy, and established the Vickers hardness prediction model of Inconel 718 by using the response surface method [17]. In addition, in the field of stone processing, Zhang et al. established a prediction model of diamond saw tooth wear rate in the process of sawing hard stone based on the response surface method [18,19]. Sun et al. used single factor and orthogonal experiment methods to study the influence of flywheel speed, block car feed speed and sawing length on the sawing force of stone. The effect of stone characteristics on vertical sawing force was studied by the response surface analysis method, realized the advance prediction of stone sawing force [20,21]. Currently, numerous studies have been conducted by scholars both domestically and internationally on the material properties and processing of various stone types [22–24]. However, there is a paucity of research concerning the development of prediction models for contour errors in Chinese character stone reliefs and the subsequent optimization of milling parameters based on these models.

This paper addresses this research gap by employing the response surface method to integrate modeling prediction and experimental analysis. Specifically, the influence of spindle speed, feed rate, milling width, and milling depth on the contour error of white marble reliefs under different processing characteristics is examined. Furthermore, based on these findings, optimal process parameters are determined, thereby providing valuable guidance for the selection of milling parameters in practical processing scenarios.

2. Stone robotic arm milling process

2.1. Experimental equipment and control software

The structure of the stone carving robotic arm is shown

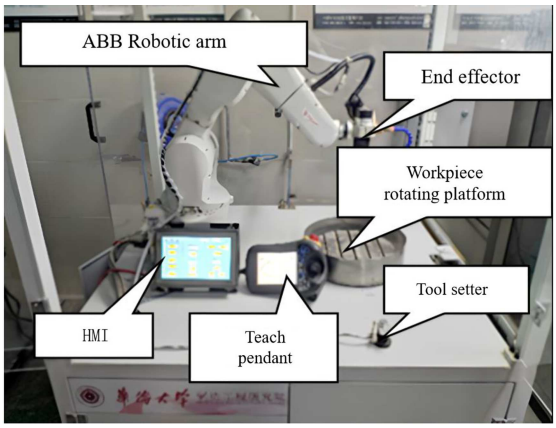

Figure 1. The system components of stone carving robotic arm.

in Figure 1. It's mainly composed of the robotic arm body (ABB1200-7 kg), the workpiece rotating platform (diameter 30 cm), the carving end effector (1.67 kg, 500 W) and the corresponding software control system. As the seventh axis of the robotic arm, the workpiece rotating platform expands the reachable space of the stone carving robotic arm processing system and facilitates the robotic arm to complete engraving tasks in different areas. The carving end effector is a terminal device used to complete engraving which is installed at the end of the robotic arm through a quick-change flange, and reaches the designated processing position with the movement of the robotic arm. The maximum working range is 703 mm, the rated load is 7 kg, and the repeated positioning accuracy is ±0.02 mm, which can be well applied to the plane relief of various types of stone.

The basic process of white marble carving by using the robotic arm is shown in Figure 2. First, the model and blank are scanned by a 3D scanner or CAD modeling, and then the established 3D model is imported into the CAM pre-processing software, setting the processing strategy and parameters, and generate tool position source files, then adjust the posture of the robot arm to generate the NC code available for the robot arm through post-processing, and import the robot arm for actual processing. In

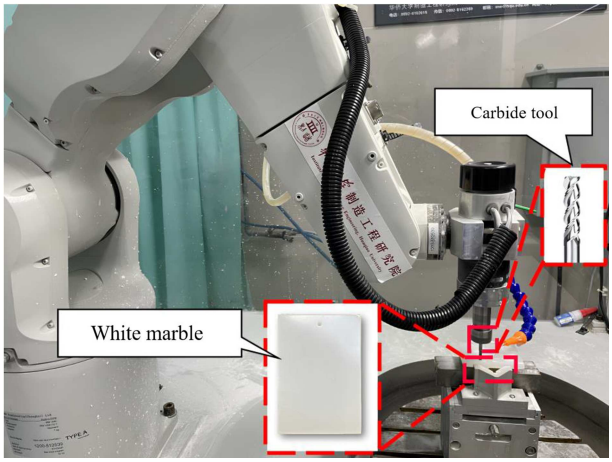

Figure 3. Experiment material and the tool for white marble milling.

stone relief processing, the contour error is usually used to characterize the processing quality. Spindle speed n, feed speed f, milling width a_e and milling depth a_p are the main process parameters that affect the contour error. The optimal combination of process parameters is the key to the best processing quality of the robotic arm carved stone.

2.2. The experimental materials and tools

In the experiment, a hard white marble with dimensions of 50 mm in length, 70 mm in width, and 8 mm in height was selected as the material for processing, as depicted in Figure 3. White marble is the most common type of rock in nature and primarily consists of quartz, orthoclase, pyroxene, and plagioclase. Quartz has the highest hardness, which is the main factor affecting the processing difficulty of white marble. The mineral composition of white marble is shown in Table 1.

Carbide tool have extremely high hardness and wear resistance, and have become the main tool for white marble processing. The final selected carbide tool in this experiment is shown in Figure 3, which is designed specifically for handling intricate details of the model., and the tool radius R is 4 mm and 2 mm. The relief of the white marble blank is completed by using

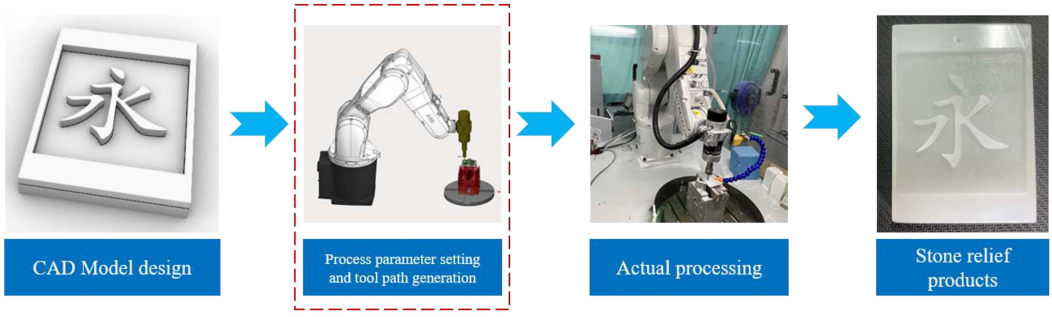

Figure 2. Stone carving robotic arm processing process.

Table 1. The main mineral composition of white marble selected in the experiment.

Chemical formula	Mineral composition	Mohs' hardness	Density (g/cm^3)	Crystal form
SiO_2	Quartz	7	$2.65-2.66$	Hexagonal
$K_2OAl_2O_36SiO_2$	Orthoclase	$6-6.5$	$2.54-2.57$	Monoclinic
$(Mg,Fe,Na)(Si,Al)_2O_6$	Pyroxene	$5-6$	$3.02-3.45$	Monoclinic
$Na(AlSi_3O_8)Ca(Al_2Si_2O_8)$	Plagioclase	$5.5-6$	$2.72-2.32$	Monoclinic

the above-mentioned carbide tools in the stone carving robotic arm processing system as shown in Figure 1.

2.3. Experimental design of milling process

Based on the "Modern Chinese Common Characters Table", this section takes the Chinese character milling in stone relief as the research object, and divides i into processing feature I: Horizontal stroke (一), feature II: Left falling stroke (丿), feature III: Horizontal turning stroke (乛), feature IV: Horizontal hook stroke (㇕) according to their outline shapes, corresponding to the four processing forms of straight line, curve, right angle, and acute angle, as shown in Figure 4.

In order to explore the influence of process parameters on the contour error Δr when the robotic arm milling different processing characteristics, n, f, a_p and a_e are defined as the independent variables, and the contour error Δr is the response variable. Based on the previous single factor test experience, the range of processing parameters is determined as follows: n is $6000-8000$ r/min, f is $300-700$ mm/min, a_p is $0.5-1$ mm, a_e is $1-2$ mm, and a 2 mm diameter milling cutter is used to ensure a certain removal rate because of the small angle of feature IV, the a_e range is set at $0.5-1$ mm. In order to display clear and easy to understand, the above uncoded variables are converted into coded variables according to Eq. (1), with A, B, C, and D representing the spindle speed n, the feed speed f, the milling depth a_p, and the milling width a_e. $+1$, 0, -1 respectively represent its high, medium, and low levels. The encoded factor levels are shown in Table 2:

$$x_i = \frac{X_i - X_0}{\Delta X}, \tag{1}$$

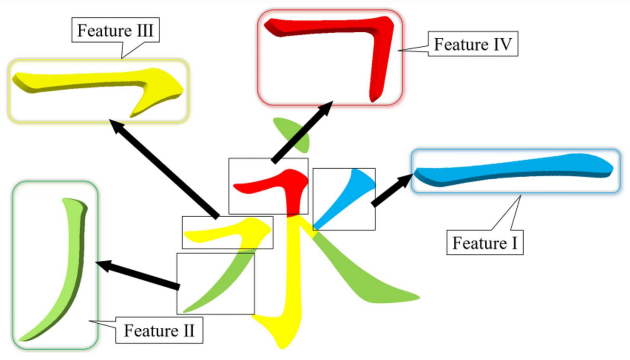

Figure 4. Characteristics division of Chinese characters.

Table 2. Coding table for the factors of white marble milling through SCRM processing.

Coding variable/level	−1	0	1
A (r/min)	6000	7000	8000
B (mm/min)	300	500	700
C (mm)	0.5	0.75	1
D (mm)	1	1.5	2

x_i is the variable code, X_i is the milling parameter variable, X_0 is the milling parameter variable zero level, ΔX is the interval change range. The Box-Behnken response surface method is used to design the experiment, and the level coding table of milling parameter factors is shown in Table 2.

2.4. Measurement of contour error

As an ornamental piece, the shape of white marble relief has an important influence on the value as an ornamental piece, and the contour error is also an important indicator of the machined quality. The machined surface contour curve is obtained by line laser scanner in Figure 5, it shows the preset model contour curve and the actual processing contour curve measured by the line laser scanner. It can be seen from the figure that it's difficult to achieve the complete coincidence of the actual machining contour and the preset model contour due to the machining errors in the machining process. The actual machining surface contour may be larger or smaller than the preset model, and there is a certain contour error, it's quantified as Δr in this figure for calculation and analysis.

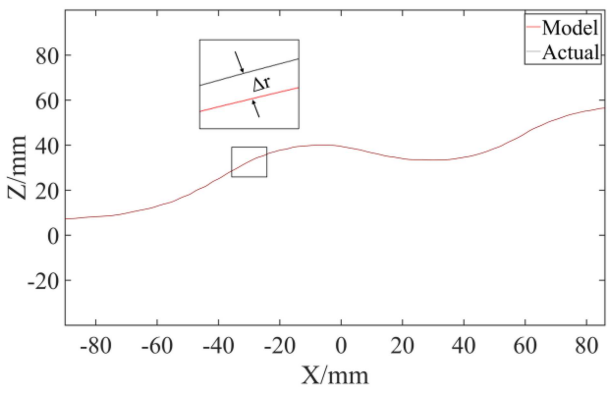

Figure 5. Schematic diagram of white marble contour curve.

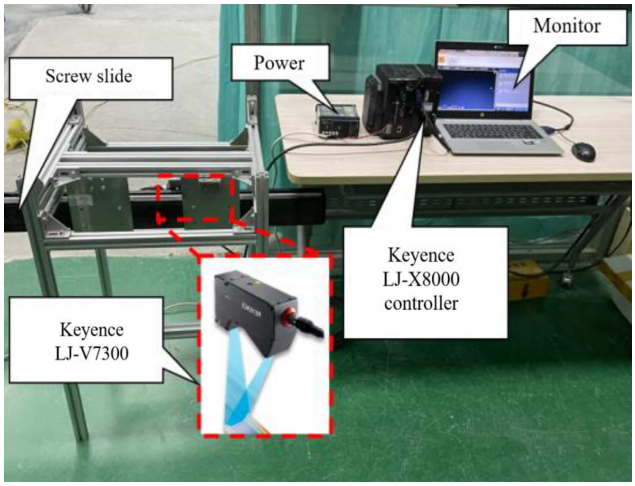

Figure 6. Schematic diagram of contour detection system.

In this paper, the contour error detection system includes three functional modules: image acquisition module, image processing module and motion control module. The image processing module is the Keyence LJ-X8000 controller; the motion control module is composed of a screw slide and a slide controller; the image acquisition module is a Keyence LJ-V7300 ultra-high-speed profile measurement sensor, which integrates with line laser transmitter and CCD camera, the measurement accuracy can reach 1 μm, as shown in Figure 6. The detection system uses the principle of laser triangulation that the laser is projected onto the object to be measured, and the three-dimensional information of the object surface is obtained through the fringe image containing the height information. First, the line laser is projected onto the object surface. After the laser line is modulated by the height of the object, the angle of the imaging beam will change, as well as the corresponding imaging position of the image on the CCD camera. As shown in Figure 7, the three-dimensional information of the object surface can be obtained by constructing the geometric structure of the optical system, analyzing the geometric structure parameters and the change of the corresponding CCD image point position.

3. Analysis and discussion of experimental results

3.1. Selection of approximate response model

RSM is a regression design that systematically combines mathematical methods, statistical principles and experimental design techniques. It is used to explore the mathematical relationship between output variables and influencing factors in the actual engineering field. The final goal is to find the optimal area and establish an optimal model to find the optimal response value and determine the influencing factor's optimal level range. Compared with the commonly used single factor method and orthogonal experiment method, RSM can systematically consider the interaction between various influencing factors and establish a higher-precision high-order polynomial regression model. The commonly used approximate models include linear models, two-factor interaction models, quadratic models, and cubic models in response surface analysis [25–27]. It shows the statistical analysis between the independent variable and the response variable and the selection of the approximate response model in Table 3. The higher-order model will not be tested since the experiment has over-fitting when using the complete cubic model. Through statistical analysis of the above four types of models, the model with the largest "correction determination coefficient R^2" and "prediction coefficient R^2" is selected as the approximate response model [28–31], it's found that the quadratic model meet the requirements when milling Feature I and Feature II, the approximate model of Feature III is a two-factor mutual relationship model; a linear model is the most suitable for Feature IV. The general formula of the model is shown in Eq. (2):

$$Y_{\Delta \mathrm{r}} = \beta_0 + \sum_{i=1}^{n} \beta_i X_i + \sum_{j \geq i}^{n} \beta_{ij} X_i X_j + \cdots + e. \qquad (2)$$

In the above formula, Y is response value, n is the number of variables, β_0 is a constant, β_i is a linear coefficient, β_{ii} is a square coefficient, β_{ij} is a product coefficient.

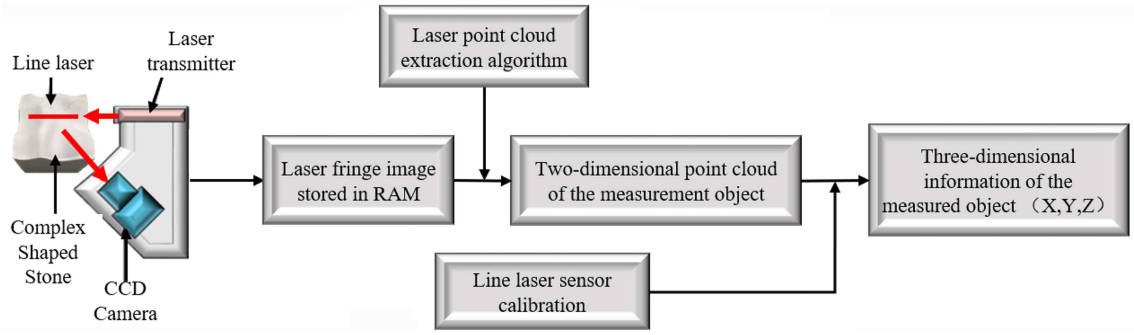

Figure 7. Diagram of principle of line laser.

Table 3. Selection of approximate response model for contour error.

Feature	Source	Standard deviation	R^2	Adjusted R^2	Predicted R^2	$P-$value	Remark
Feature I	Linear	0.0066	0.9362	0.9255	0.9023	0.0016	
	2FI	0.0067	0.9506	0.9231	0.8465	0.0025	
	Quadratic	0.0031	0.9917	0.9834	0.9626	0.0006	Suggested
	Cubic	0.0029	0.9970	0.9859	0.9244	0.0012	Aliased
Feature II	Linear	0.0071	0.9345	0.9236	0.9006	0.0018	Suggested
	2FI	0.0079	0.9396	0.9060	0.8143	0.0034	
	Quadratic	0.0054	0.9774	0.9549	0.8848	0.0021	Suggested
	Cubic	0.0051	0.9914	0.9599	0.2654	0.0135	Aliased
Feature III	Linear	0.0155	0.8502	0.8252	0.7694	0.0088	
	2FI	0.0114	0.9387	0.9046	0.8152	0.0071	Suggested
	Quadratic	0.0113	0.9533	0.9066	0.7543	0.0094	
	Cubic	0.0074	0.9914	0.9596	0.5474	0.0173	Aliased
Feature IV	Linear	0.0127	0.8854	0.8663	0.8270	0.0058	Suggested
	2FI	0.0122	0.9207	0.8767	0.7670	0.0079	
	Quadratic	0.0111	0.9487	0.8975	0.7269	0.0092	
	Cubic	0.0115	0.9767	0.8912	–1.6025	0.0879	Aliased

3.2. Significance analysis of regression coefficients

The corresponding approximate response model of the contour error is created in the Design Expert12™ software after determining, and obtain the variance analysis results of different processing features as shown in Table 4 to Table 7. The P value in the table is a probability, which is used to measure the evidence for negating the null hypothesis. The lower the probability, the more sufficient evidence to deny the null hypothesis. The P value is used to determine whether the null hypothesis can be rejected or not, and show that there is no association between the two categorical variables. It indicates that the model or factor has a significant impact when P<0.05, the model or factor is considered to have a low impact as the P>0.10. Removing low-impact items (excluding items that support the model structure and research in this paper) and simplifying the model can improve the approximate response model.

According to Table 4, the influence of B, C, D on the contour error when milling the feature I is extremely significant ($P < 0.0001$), and the influence of CD, A^2, B^2, C^2, D^2 is more significant ($P < 0.05$), the others are not significant. The order of the process parameters affecting the feature I contour error is $C > D > B > A$ according to the comparison of the magnitude of the mean square error. And there is no lack of fit item in this table, which proves that the response surface and its representative regression equation are reliable.

In Table 5, the F value of the model is 43.32, and its P value means the corresponding probability is less than 0.01%, indicating that the model is extremely significant. In addition, the B-C-D-A^2-D^2 are the significant items in the mathematical model of the feature II contour error. By comparing the magnitude of the mean square error, it's known that the process parameters affect the feature II contour error are ranked as follows: $C > D > B$.

As shown in Table 6, the P value of items C and D indicates that these two items have a very significant impact on the feature III contour error, the effects of A, B, and CD are more significant ($P < 0.05$), the others are not significant. According to the comparison of the magnitude of the mean square error, the order of the process parameters affecting the Feature III contour error is $D > C > B > A$.

It can be obtained that the items B, C, and D are significant items of the feature IV contour error from Table 7. The rank of each process parameter influence is D>C>B, and the lack of fit of the response

Table 4. The significance analysis of contour error parameters of feature I.

Source	Sum of fquares	Degree of freedom	Mean square	F-value	P-value $Prob > F$
Model	0.0161	14	0.0012	119.22	< 0.0001 significant
$A - n$	0.0000	1	0.0000	3.46	0.0842
$B - f$	0.0004	1	0.0004	38.78	< 0.0001
$C - a_p$	0.0102	1	0.0102	1052.21	< 0.0001
$D - a_e$	0.0046	1	0.0046	481.15	< 0.0001
AB	4.000E–06	1	4.000E-06	0.4147	0.5300
AC	4.000E–06	1	4.000E–06	0.4147	0.5300
AD	1.000E–06	1	1.000E–06	0.1037	0.7522
BC	9.000E–06	1	9.000E–06	0.9330	0.3505
BD	6.250E–06	1	6.250E–06	0.6479	0.4343
CD	0.0002	1	0.0002	21.80	0.0004
A^2	0.0002	1	0.0002	24.34	0.0002
B^2	0.0001	1	0.0001	8.76	0.0104
C^2	0.0001	1	0.0001	14.28	0.0020
D^2	0.0001	1	0.0001	12.05	0.0037
Residual	0.0001	14	9.646E–06		
Lack of fit	0.0001	10	9.425E–06	0.9240	0.5844 not significant
Pure error	0.0000	4	0.0000		
Cor total	0.0162	28			

Table 5. The significance analysis of contour error parameters of feature II.

Source	Sum of fquares	Degree of freedom	Mean square	F-value	P-value $Prob > F$
Model	0.0180	14	0.0013	43.32	< 0.0001 significant
$A - n$	0.0001	1	0.0001	1.76	0.2059
$B - f$	0.0005	1	0.0005	17.57	0.0009
$C - a_p$	0.0127	1	0.0127	430.34	< 0.0001
$D - a_e$	0.0039	1	0.0039	130.12	< 0.0001
AB	0.0000	1	0.0000	0.6840	0.4221
AC	0.0000	1	0.0000	1.02	0.3292
AD	2.500E-07	1	2.500E-07	0.0084	0.9281
BC	6.250E-06	1	6.250E-06	0.2111	0.6529
BD	6.250E-06	1	6.250E-06	0.2111	0.6529
CD	0.0000	1	0.0000	1.02	0.3292
A^2	0.0002	1	0.0002	6.57	0.0226
B^2	0.0001	1	0.0001	3.12	0.0990
C^2	0.0001	1	0.0001	3.12	0.0990
D^2	0.0002	1	0.0002	7.95	0.0136
Residual	0.0004	14	0.0000		
Lack of fit	0.0003	10	0.0000	2.16	0.2385 not significant
Pure error	0.0001	4	0.0000		
Cor total	0.0184	28			

Table 6. The significance analysis of contour error parameters of feature III.

Source	Sum of fquares	Degree of freedom	Mean square	F-value	P-value $Prob > F$
Model	0.0360	10	0.0036	27.55	< 0.0001significant
$A - n$	0.0006	1	0.0006	4.72	0.0434
$B - f$	0.0008	1	0.0008	5.76	0.0274
$C - a_p$	0.0077	1	0.0077	59.01	< 0.0001
$D - a_e$	0.0235	1	0.0235	180.05	< 0.0001
AB	2.250E–06	1	2.250E–06	0.0172	0.8970
AC	0.0000	1	0.0000	0.3237	0.5764
AD	0.0000	1	0.0000	0.2759	0.6058
BC	0.0001	1	0.0001	0.6207	0.4410
BD	0.0000	1	0.0000	0.2759	0.6058
CD	0.0032	1	0.0032	24.46	0.0001
Residual	0.0023	18	0.0001		
Lack of fit	0.0021	14	0.0002	2.86	0.1599 not significant
Pure error	0.0002	4	0.0001		
Cor total	0.0383	28			

Table 7. The significance analysis of contour error parameters of feature IV.

Source	Sum of fquares	Degree of freedom	Mean square	F-value	P-value $Prob > F$
Model	0.0299	4	0.0075	46.35	< 0.0001 significant
$A - n$	0.0002	1	0.0002	1.19	0.2860
$B - f$	0.0022	1	0.0022	13.90	0.0010
$C - a_p$	0.0091	1	0.0091	56.63	< 0.0001
$D - a_e$	0.0183	1	0.0183	113.69	< 0.0001
Residual	0.0039	24	0.0002		
Lack of fit	0.0037	20	0.0002	4.13	0.0890 not significant
Pure error	0.0002	4	0.0000		
Cor total	0.0338	28			

surface and its representative regression equation is not significant.

3.3. The establishment of contour error prediction model

In order to obtain the optimal regression equation between the process parameters and the contour error, the insignificant items in Tables 4 to 7 are deleted, and establish the final response surface model of the contour error under different processing characteristics respectively, are shown in Eqs. (3)–(6). The established model can be used to effectively predict the contour error when the robotic arm is milling white marble.

$$\begin{aligned}\Delta r_I =& 0.0972 + 0.0017A + 0.0056B + 0.0291C \\ &+ 0.0197D + 0.0073CD - 0.006A^2 \\ &+ 0.0036B^2 + 0.0046C^2 + 0.0042D^2, \end{aligned} \tag{3}$$

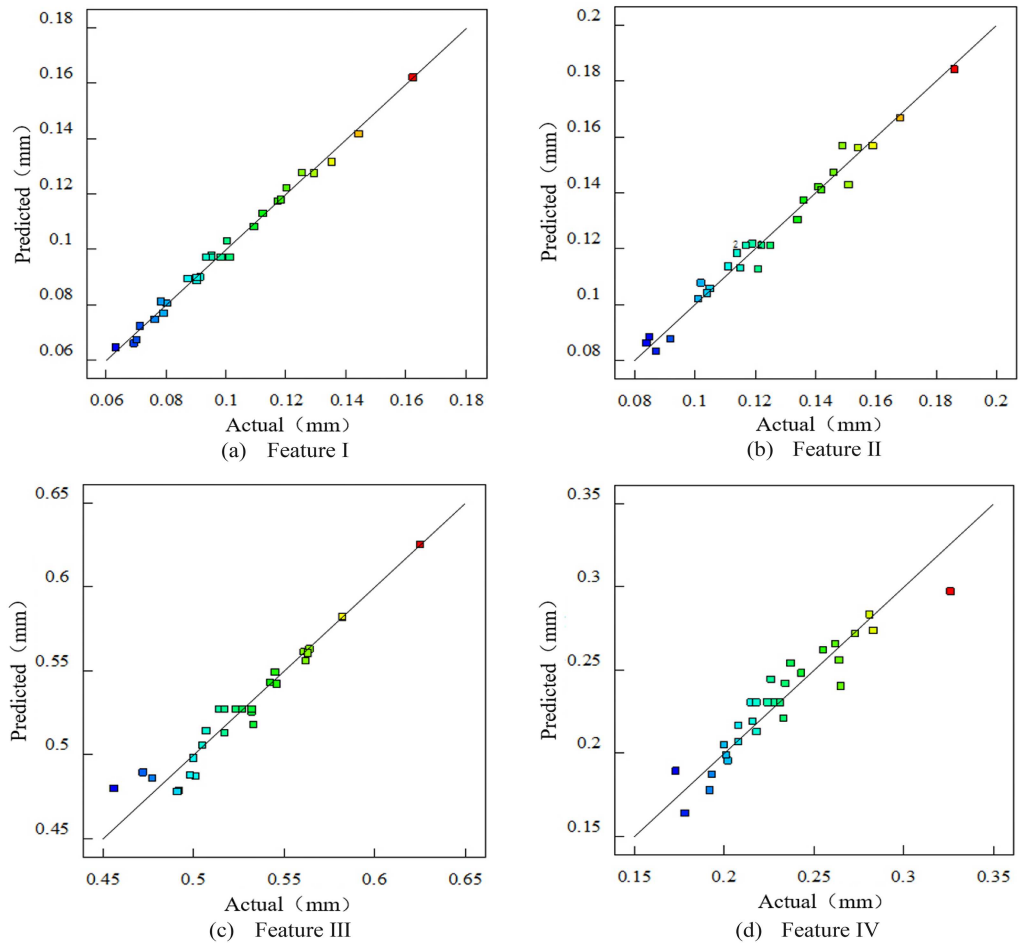

Figure 8. Comparison between the predicted and actual values of various machining feature profile errors.

Table 8. Coefficient comparison of the two contour error models.

Name feature	Std. dev.	Mean value	C.V.%	R^2	Adjusted R^2	Predicted R^2	Adeq. precision
Feature I	0.0029	0.0999	2.90	0.9902	0.9855	0.9778	57.3420
Feature II	0.0055	0.1246	4.41	0.9639	0.9540	0.9379	37.4357
Feature III	0.0105	0.5272	2.00	0.9335	0.9191	0.8594	31.3402
Feature IV	0.0127	0.2306	5.53	0.8797	0.8653	0.8309	28.1665

$$\Delta r_{II} = 0.1253 + 0.0021A + 0.0066B + 0.0326C + 0.0179D - 0.0067A^2 + 0.0048D^2, \quad (4)$$

$$\Delta r_{III} = 0.5272 + 0.0072A + 0.0079B + 0.0253C + 0.0442D + 0.0282CD, \quad (5)$$

$$\Delta r_{IV} = 0.2306 + 0.0137B + 0.0276C + 0.0391D. \quad (6)$$

The standard deviation and determination coefficient of the final response surface model are shown in Table 8. The model with stronger explanatory power, higher reliability and fitting degree can be obtained by eliminating the insignificant items. From the table, it can be seen that the response surface equation has high prediction accuracy. The "Predicated R^2" and the "Adjusted R^2" both are close to 1, and the difference between them is less than 0.2. In summary, the prediction model established for each processing feature is reliable.

3.4. Model validity verification

Figure 8(a)–(d) are the comparison diagrams about the actual and predicted values of the four processing feature contour errors. It can be seen from the figure that the points of the actual value and the predicted value are basically distributed near the diagonal, indicating that the prediction residuals of each response can be ignored, the predicted value and the actual value

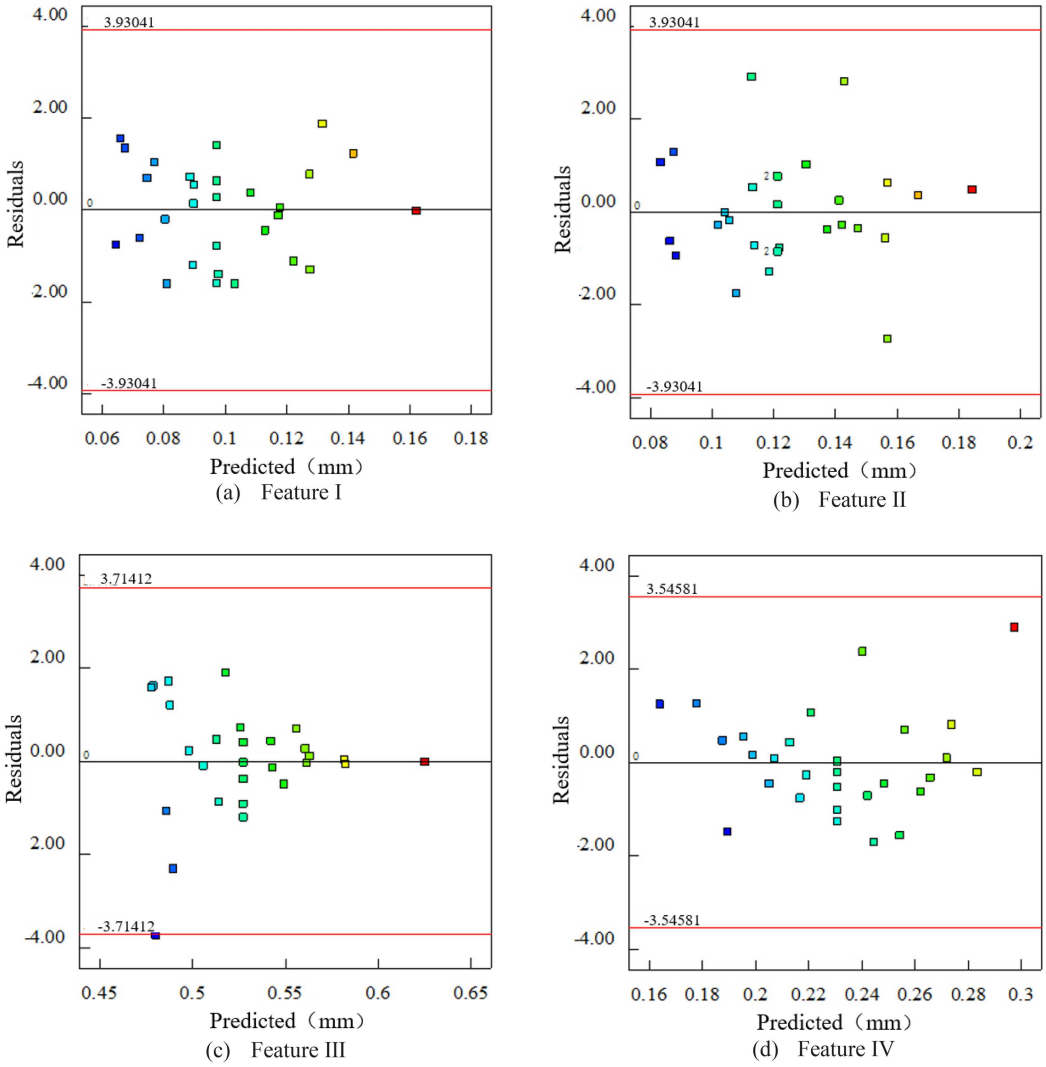

Figure 9. Correlation distribution diagram between residual and predicted values of various processing feature.

are not much different, and the model fit well. The points in Figure 9 distribute randomly, it shows that the residuals and predicted values are irrelevant, and further verifies the reliability of the model established.

Fix some of the two factors at the intermediate level, so as to analyze the interaction effects of the other two factors on the evaluation index. Analyze the influence of the four process parameters on the contour error by making the influence trend graph and the response surface graph.

3.4.1. Analysis about the influence of process parameters on the feature I contour error

It shows the influence of each process parameter on the feature I contour error in Figure 10. It can be seen that the milling depth has the greatest influence, the second is the milling width, followed by the feed rate, and the spindle speed has the least influence. With the increase of milling depth, milling width and feed rate, the contour error increases. For the increase of

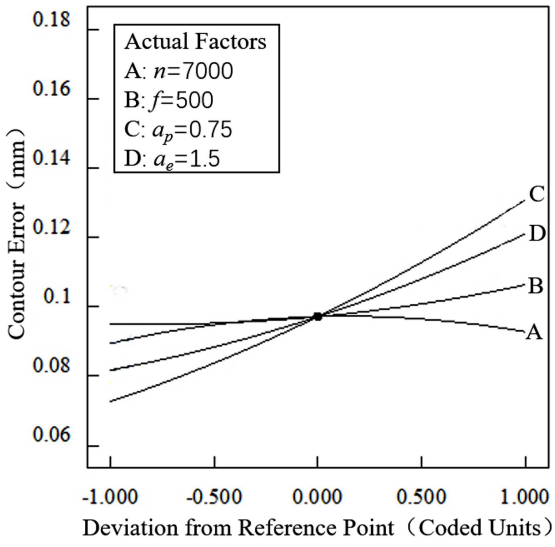

Figure 10. The process parameters for processing feature I contour error influence trend chart.

the spindle speed, the contour error first increases and then decreases.

The response surface graph is a three-dimensional space surface graph composed of each influencing factors and response values. The interaction relationship between each process parameters and the best parameter combination can be obtained according to the graph. Figure 11 is the surface graph about the influence of each process parameters on the feature I contour error.

In Figure 11(a), (b), and (c), it can be seen that as the spindle speed increases, the contour error shows a trend from rise to decline. The tool wears sharply with the increasing spindle speed, it is the reason of the contour error changes. When the speed reaches 7000 r/min, the tool vibration tends to be stable, so the contour error decreases.

According to Figure 11(a), (d), and (e), the contour error rises as the feed rate increases. The reason is the material removal rate and tool deformation grow accordingly, the tool load becomes larger, vibration occurs, and the cutting force required for material removal increases. It also causes the chips become larger, intensifies the friction between the tool and the cutting.

Figure 11(b), (d), and (f) show that the contour error is positively correlated milling depth. It can be understood an increase in milling width leads to the larger contact area between tool and workpiece, increased friction and the continuous high temperature of the cutting area intensify the wear of the tool and affects the contour accuracy of the workpiece.

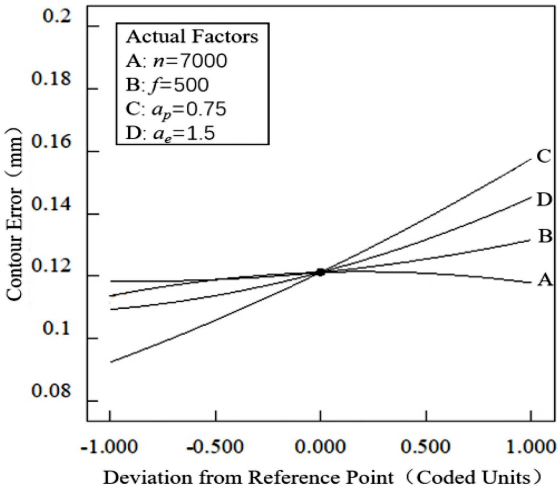

Figure 12. The process parameters for processing feature II contour error influence trend chart.

From Figure 11(c), (e), and (f), the trend between milling width and contour error is roughly the same as that of milling depth. With the milling width increases, the deformation of the workpiece and the material removal rate increase accordingly, which intensifies the load of the robotic arm, causes the chips to become larger, and ultimately leads to the constantly decline of machining accuracy.

3.4.2. Analysis about the influence of process parameters on the feature II contour error

Through the Figure 12, it can be obtained that the feature II contour error rises with the increase of feed

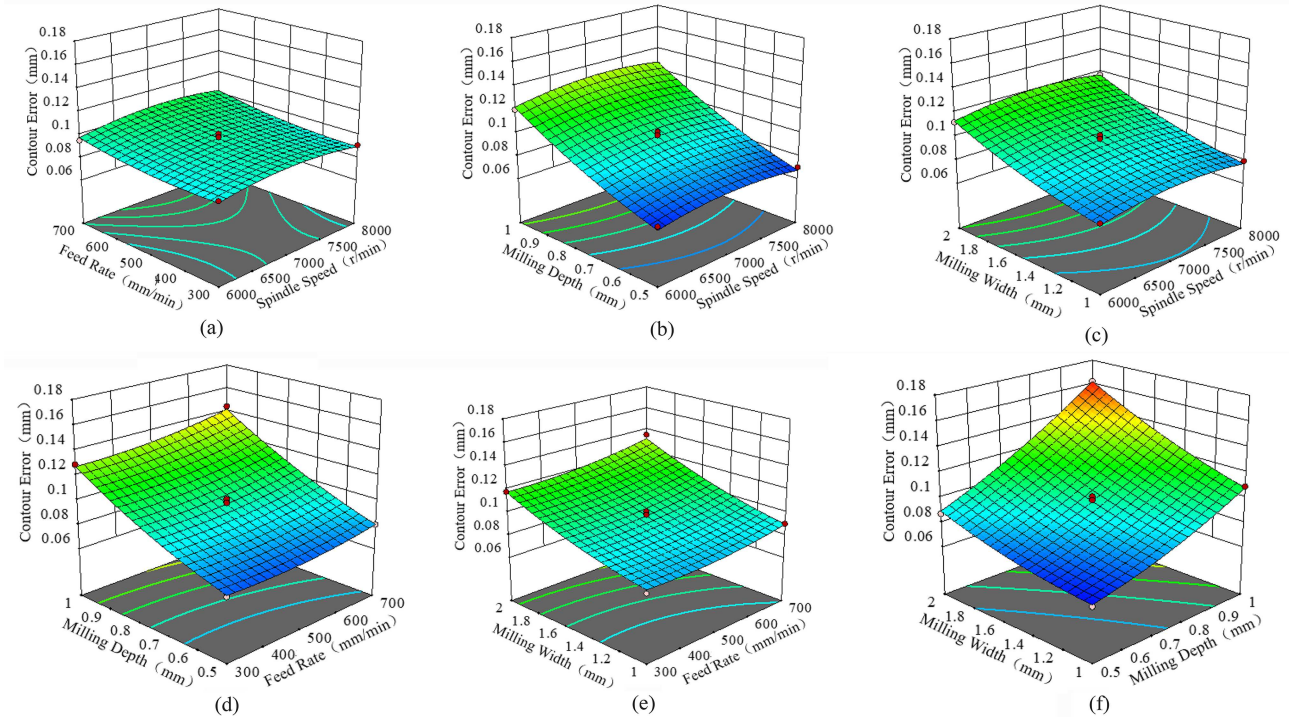

Figure 11. The response surface of the contour error (feature I).

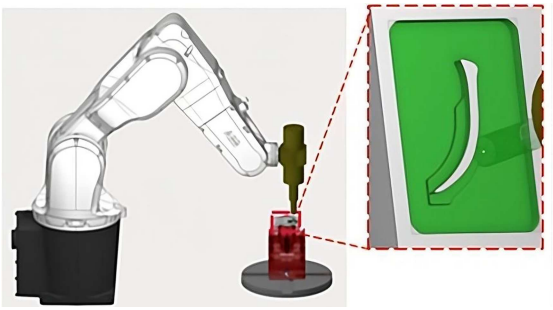

Figure 13. Machining features II bend.

rate, milling width and milling depth, while the spindle speed has little effect on it. The influence trend of each parameter on the feature II contour error is roughly the same as that of feature I, but the contour error is overall larger than that of it. This is because the feature II contour has a certain curvature, which is similar to curve machining (as shown in Figure 13), makes the force on tool become larger, increases the tool movement and tool wear at the same time.

Figure 14 shows the three-dimensional variation diagram between the feature II contour error and different machining process parameters.

3.4.3. Analysis about the influence of process parameters on the feature III contour error

As shown in Figure 15, the feature III contour error increases with the growth of the processing parameters. The milling width has a greatest influence, the spindle

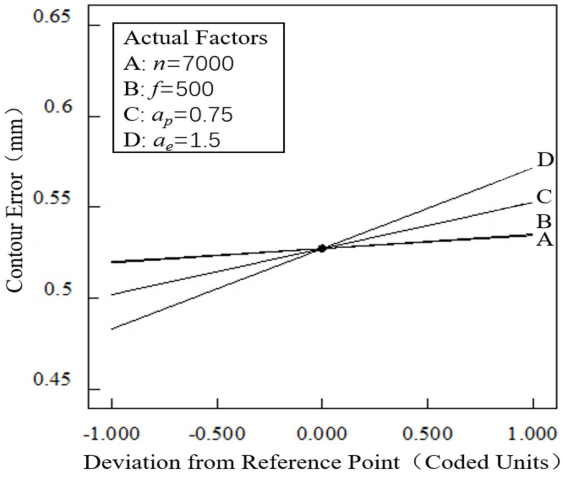

Figure 15. The process parameters for processing feature III contour error influence trend chart.

speed and the feed rate less affected. Compared with the first two features, the effect of spindle speed no longer shows a trend from rise to decline, and the milling width becomes the main influencing factor. The corners in feature III causes a sudden trajectory change, so the increasing milling width makes the processing collapse serious. The growth of overall feature III contour error due to the area with a curvature less than the tool diameter at the corner, as shown in Figure 16, which makes the tool unable to process to this part.

There is the three-dimensional variation diagram

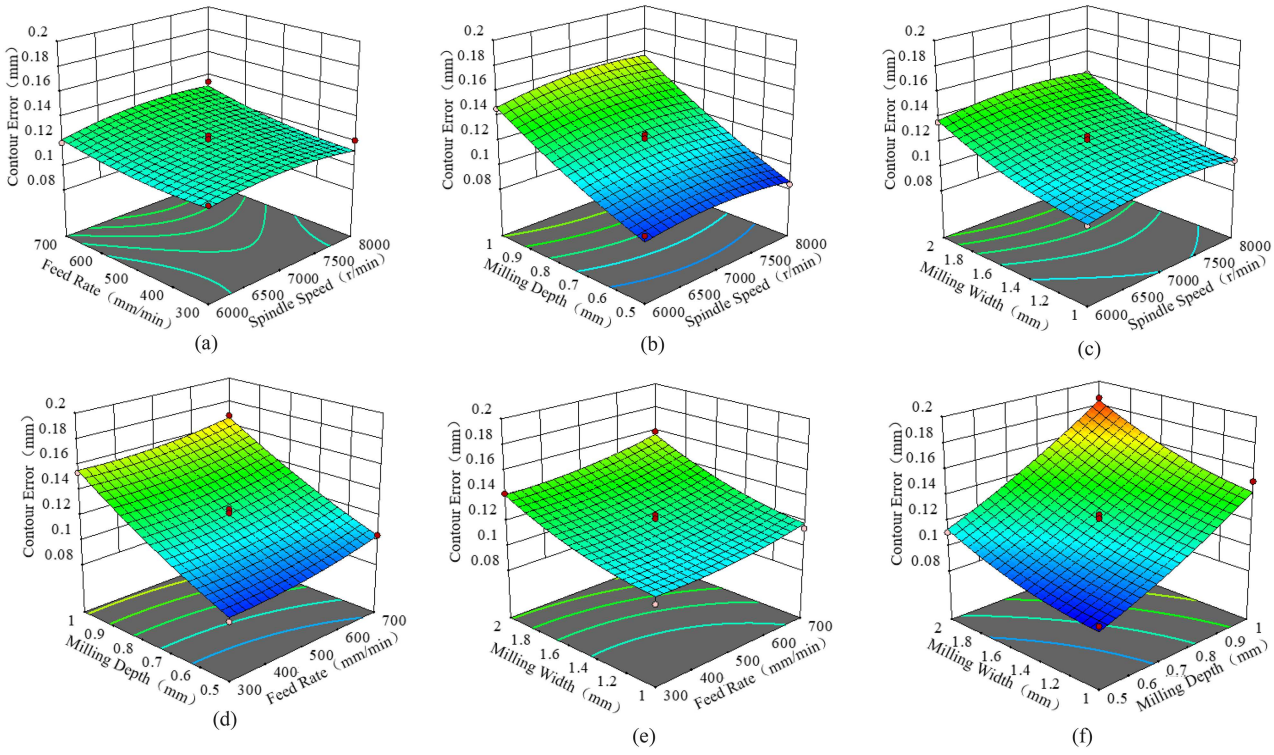

Figure 14. The response surface of the contour error (feature II).

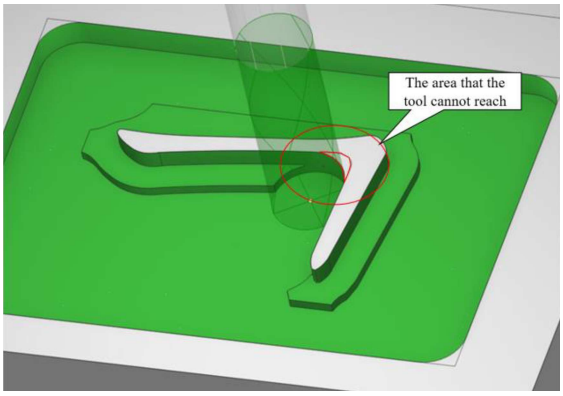

Figure 16. Machining features III corner.

and the single-factor influence variation diagram about the effect of different processing parameters on the feature III contour error in Figure 17.

3.4.4. Analysis about the influence of process parameters on the feature IV contour error

As shown in Figure 18, it can obtain that each processing parameters are positively correlated with feature IV contour error, the influence of the feed rate is significantly greater than that of feature IV due to the smaller angle at the feature IV corner and the larger path abrupt change, making the contour error change more sensitive to the feed rate, and the workpiece is more susceptible to chipping, but the milling width is still the main influencing factor. Although this feature uses a smaller diameter tool, there are also an area that the tool cannot reach as shown in Figure 19, resulting in a relatively large overall contour error.

In Figure 20, the influence of each factor on the contour error in this feature is independent, and there is no obvious interaction between the two of them.

4. Analysis and discussion of experimental results

The experiment data are optimized and analyzed in Design Expert 12, including the design of the optimization objective function, the optimization variables and the constraint conditions, it must be satisfied that a desired optimization achieved under the given experimental conditions when establishing the model. The main goal of robotic arm milling white marble

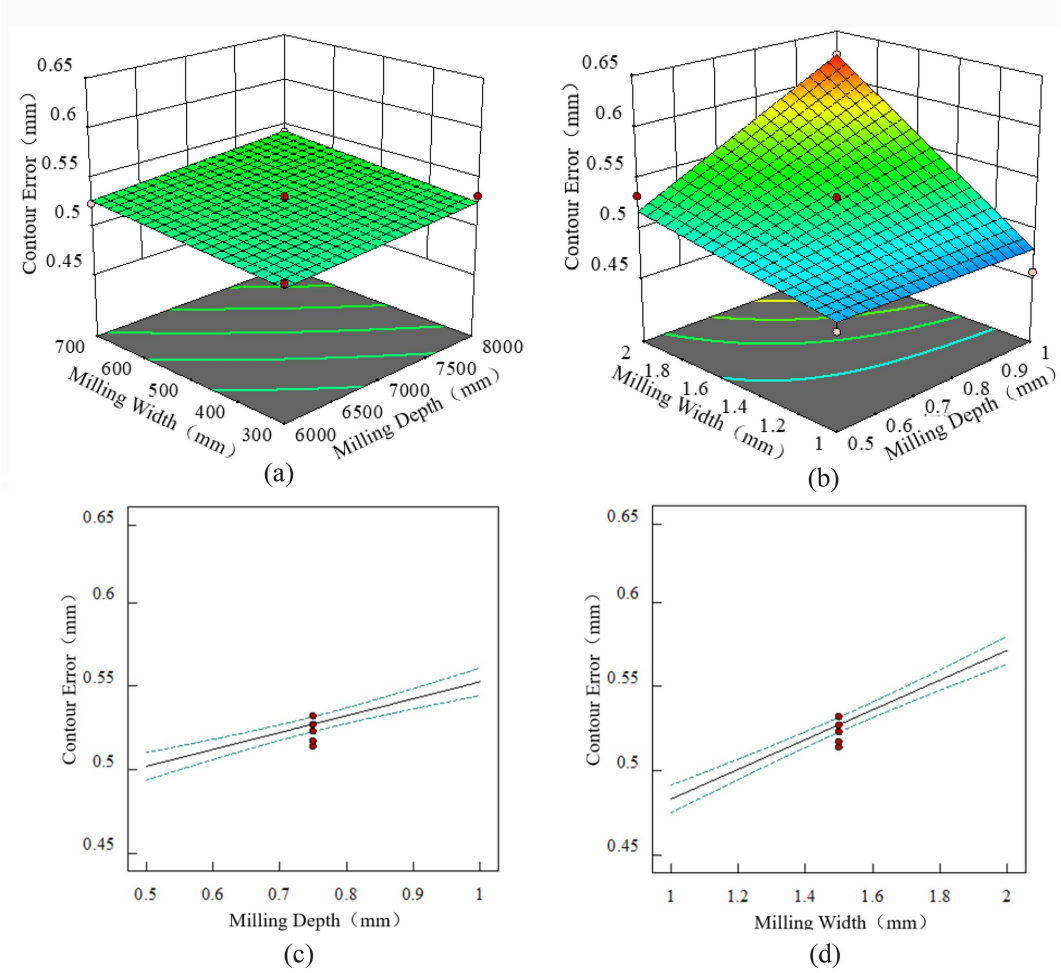

Figure 17. The response surface of the contour error (feature III).

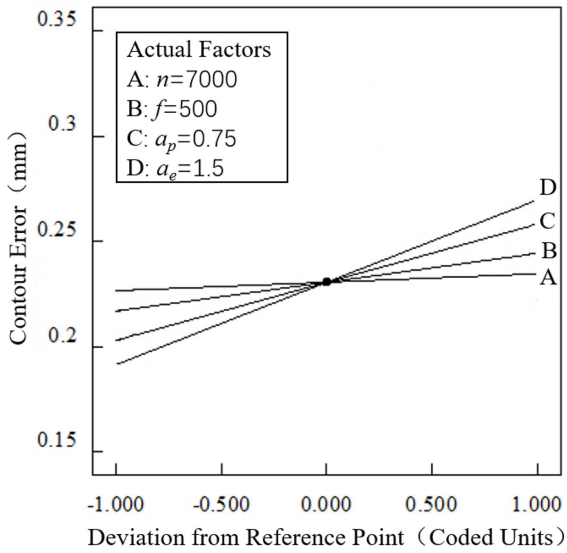

Figure 18. The process parameters for processing feature IV contour error influence trend chart.

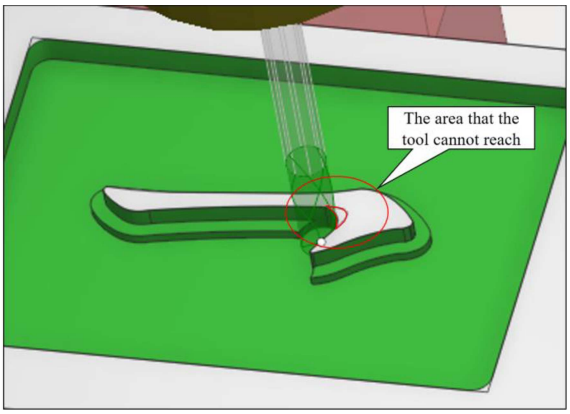

Figure 19. Machining features IV corner.

relief products is to minimize the contour error of the workpiece under the existing conditions. In the optimization process design, it's necessary to determine the appropriate optimization variables first. The more optimized parameters, the greater the freedom degree, which is more conducive to the solution of the problem. However, too many optimized parameters may make the solution too difficult. According to the actual processing conditions, the processing parameters n, f, a_p, and a_e are used as optimization variables.

In actual processing, the optimization of processing parameters is affected by many factors, such as equipment, tools and processing quality. Therefore, it's necessary to limit the range of process parameters. Thinking about the feature selection of process parameters, the small force and power in milling process, there is no need to individually constrain them, but the limitations of the manipulator body and the tool and the requirements for processing quality are considered in design. Table 9 shows the optimization constraints of each machining feature experiment. The inputs are set within a certain range, and all the parameters and responses are given the same weight and importance. Satisfaction analysis is performed on the inputs, and the minimum contour error rate is the optimization objective function.

Through reasonable experimental analysis, it can be obtained that the optimal solution of the parameter combination, the prediction of the contour error and desirability for each processing feature from Table 10. The expected bar graph for each optimal solution is shown in Figure 21. The parameter factors are set in the first 4 bars, and the best expected response value is displayed in the remaining bars.

In order to further verify the actual processing result of the above optimization method, a set of control experiments were carried out. According to the optimized process parameter combinations of different processing features obtained in Table 10, the word "?" is processed in partitions with the division method shown in Figure 4. Another set of control experiments will use traditional single process parameters to engrave (n = 7000 r/min, f = 500 mm/min, a_p = 0.75 mm, a_e = 0.75 mm). The control experiment results

Table 9. Range of input parameters and response (feature I, II, III, IV).

Name	Goal	Lower limit	Upper limit	Lower weight	Upper weight	Importance
$A : n$	Is in range	6000	8000	1	1	3
$B : f$	Is in range	300	700	1	1	3
$C : a_p$	Is in range	0.5	1	1	1	3
$D : a_e$	Is in range	1	2	1	1	3
Feature I Δr	Minimize	0.063	0.162	1	1	3
Feature II Δr	Minimize	0.084	0.186	1	1	3
Feature III Δr	Minimize	0.456	0.625	1	1	3
Feature IV Δr	Minimize	0.173	0.326	1	1	3

are shown in Figures 22 and 23, and the numerical comparison of processing time and contour error is shown in Figure 24.

According to the comparison of Figures 22 and 23, it is obvious that the processing quality of the optimized processing is significantly better than the traditional processing method. There are obvious fragmentations at some stroke features in traditional processing method due to the mismatch of parameters, and the optimized processing workpiece has no obvious damage. From the bar graph of Figure 24, although the processing time of optimized processing compared

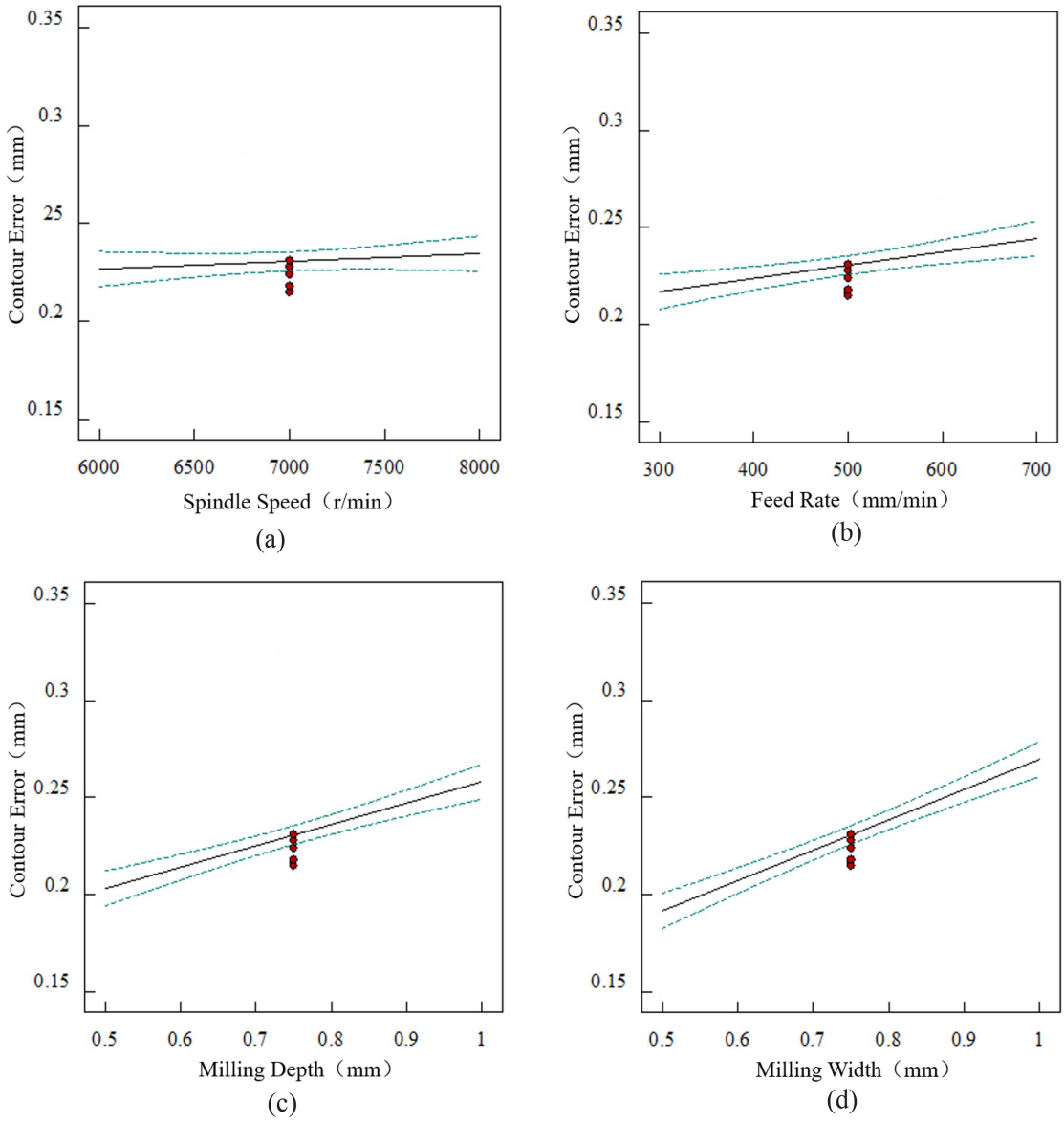

Figure 20. The response surface of the contour error (feature IV).

Table 10. Parameter optimization results.

Number	n (r/min)	f (mm/min)	a_p (mm)	a_e (mm)	Δr (mm)	Desirability
Feature I	7916.462	317.171	0.514	1.044	0.060	0.989
Feature II	6802.833	451.436	0.505	1.135	0.084	0.880
Feature III	6644.944	444.439	0.801	1.000	0.480	0.817
Feature IV	7788.015	310.131	0.505	0.520	0.158	0.900

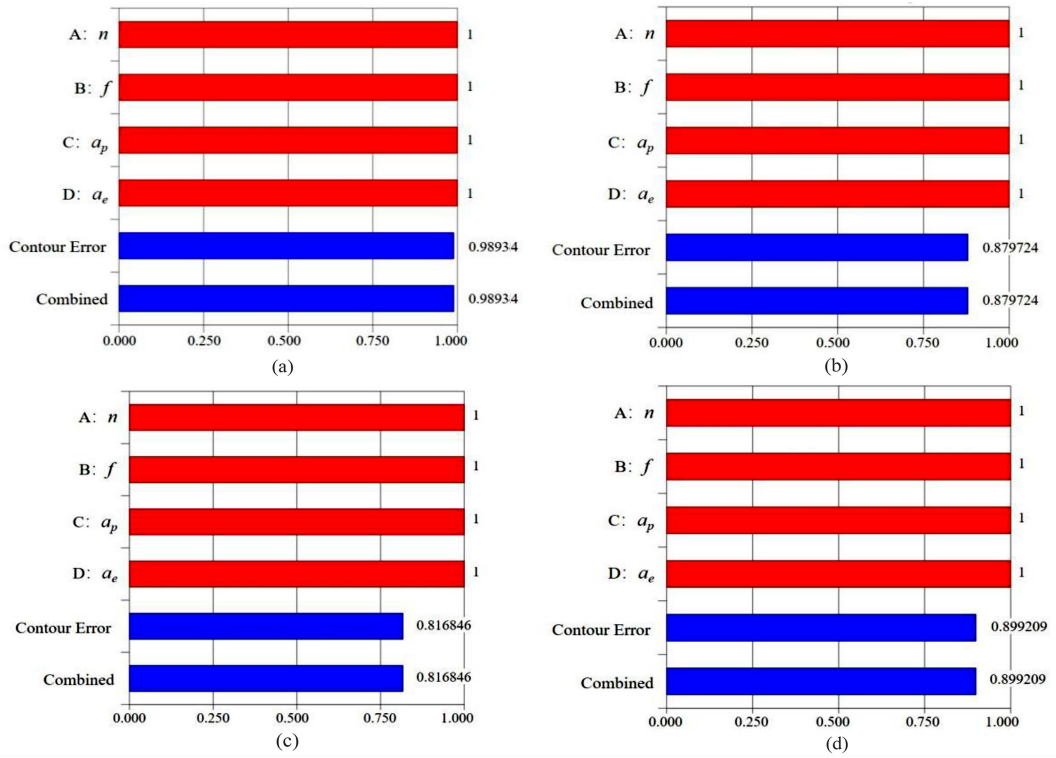

Figure 21. Compound desirability bar graph.

with the traditional processing has been increased by 13%, but the contour error has been reduced by 47%. Therefore, the feature partitioning processing method of Chinese character relief is significantly better than the traditional method in terms of quality, and this control experiments also further proves the effectiveness of the optimized method in this paper.

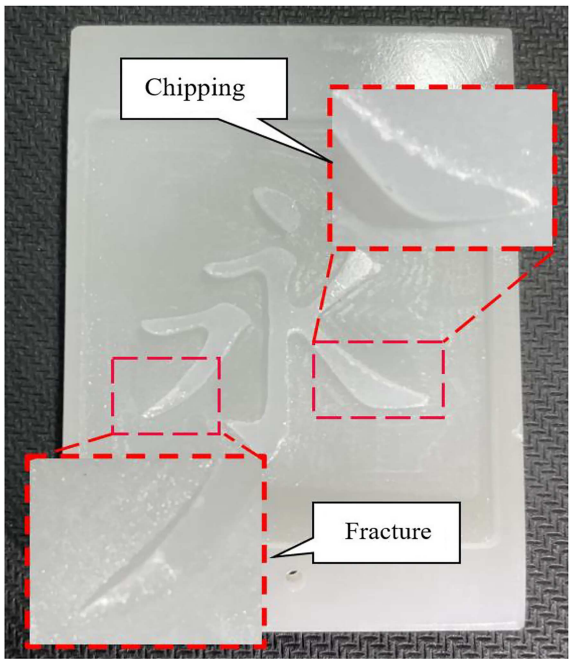

Figure 22. Traditional processing results.

5. Conclusions

1. This study focused on Chinese character stone relief as the research object and proposed a feature partitioning milling method for it in robotic arm based on its different contour features. The Chinese character relief was divided into four typical processing features according to their outline shapes, feature I: Horizontal stroke (㇐), feature II: Left falling stroke (丿), feature III: Horizontal turning stroke (乛), feature IV: Horizontal hook stroke (亅), which correspond to four different machining forms: straight line, curve, right angle, and acute angle. Optimal process parameters for each processing feature were obtained through experiments. The experimental results showed that compared to traditional single-parameter carving processes, using this method increases processing time by 13%, but reduces the contour error by 47%, significantly improving the processing quality of robotic arm milling on Chinese white marble;
2. The response surface methodology was employed to investigate the effects of key milling parameters, including spindle speed, feed speed, milling depth, and milling width, on the contour error of Chinese white marble under different processing features. Prediction models for the contour error of Chinese character white marble relief under different pro-

Figure 23. Optimized machining results.

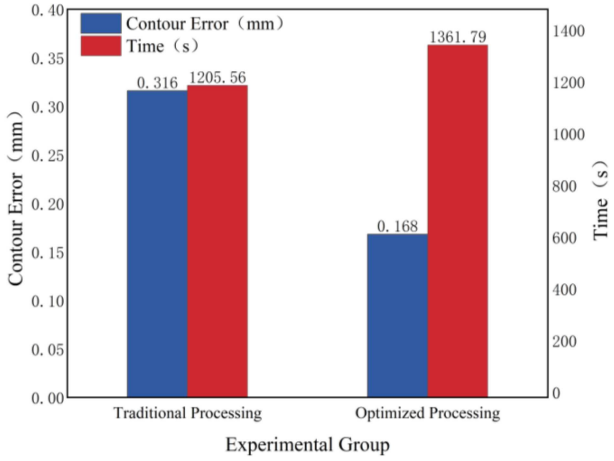

Figure 24. Contrast of traditional processing and optimized processing.

cessing features were established. Based on the data analysis results, the quadratic model proved to be more reliable in predicting the contour error of stone relief features I and II. For feature III, a two-factor interaction model was found to be most suitable. As for feature IV, a linear model was deemed more reliable;

3. Through the response surface analysis, the order of the influence and trend between the milling parameters and each feature contour error was reflected intuitively. It showed that the milling depth has the greatest influence on the contour error for feature I, followed by the milling width, the next is feed rate, and the spindle speed is the least affected. For feature II, it's roughly the same as that of feature I. In feature III, the milling width becomes the main influencing factor, and the effect of spindle speed no longer shows a trend from rise to decline compared with the first two features. The influence order of the process parameters on feature IV contour error is: milling width > milling depth > feed rate > spindle speed.

Acknowledgment

This work was supported by Major Industry-University-Research Projects in Fujian Province (Grant No.2022H6029) and Fujian Science and Technology Project (Grant No.2022H0018). The authors would like to thank the sponsor for this support. YFC would acknowledge the support from the "Promotion Program for Young and Middle-aged Teacher in Science and Technology Research of Huaqiao University".

Nomenclature

n	Spindle speed (r/min)
f	Feed speed (mm/min)
a_p	Milling depth (mm)
a_e	Milling width (mm)
x_i	Variable code
X_i	Variable
X_0	Variable zero level
ΔX	Interval change range
Δr	Contour error value (mm)
Y	Response value
n	Number of variables
β_0	Constant
β_i	Linear coefficient
β_{ii}	Square coefficient
β_{ij}	Product coefficient
Δr_I	Response value of feature I
Δr_{II}	Response value of feature II
Δr_{III}	Response value of feature III
Δr_{IV}	Response value of feature IV
CCD	Charge Coupled Device
RSM	Response Surface Methodology
feature I	Horizontal stroke (—)
feature II	Left falling stroke (丿)
feature III	Horizontal turning stroke (ㄱ)
feature IV	Horizontal hook stroke (→)

References

1. Unger, K. "Carving his own unique niche", In *Symbols and Stone, Science*, **314**(5798), pp. 412–413 (2006). DOI: 10.1126/science.314.5798.412
2. Alexander, V., Anna, V., and Shreyes, M. "Robots

in machining", *CIRP Annals-Manufacturing Technology*, **68**, pp. 799–822 (2019). DOI: 10.1016/j.cirp.2019.05.009

3. Shaked, T., Sinai., K.B., and Sprecher, A. "Adaptive robotic stone carving: Method, tools, and experiments", *Automation in Construction*, **129**, p. 103809 (2010). DOI: 10.1016/j.autcon.2021.103809
4. Wang, J., Huang, S.G., Huang , J.X., et al. "Parameter analysis and modelling of grinding complex-shaped granite by diamond tools based on a robot stone machining system", *Int J Abra Tech*, **10**(1), pp. 62–82 (2020). DOI: 10.1504/IJAT.2020.109617
5. Yuan, L., Pan, Z.X., Ding, D.H., et al. "A review on chatter in robotic machining process regarding both regenerative and mode coupling mechanism", *IEEE/ASME Transactions on Mechatronics*, **23**(5), pp. 2240–2251 (2018). DOI: 10.1109/TMECH.2018.2864652
6. Yin, F.C., Ji, Q.Z., and Wang, C.Z. "Research on machining error prediction and compensation technology for a stone-carving robotic manipulator", *International Journal of Advanced Manufacturing Technology*, **115**, pp. 1683–1700 (2021). DOI: 10.1007/s00170-021-07230-z
7. Xiong, Q.Q., Wang, J.X., and Zhou, Q.H. "Prediction model of machining errors based on precision and process parameters of machine tools", *Acta Aeronautica et Astro-nautica Sinica*, **39**(8), pp. 267–275 (2018). DOI: 10.7527/S1000-6893.2018.21713
8. Wang, X.S., Kang, M., and Fu, X.H. "Prediction model of surface roughness in lenses precision turning", *Journal of Mechanical Engineering*, **49**(15), pp. 192–198 (2013). DOI: 10.1007/s00170-013-5231-3
9. Han, J.H. and Requicha, A.A. "Integration of feature based design and feature recognition", *Computer-Aided Design*, **29**(5), pp. 393–403 (1997). DOI: 10.1016/S0010-4485(96)00079-6
10. Muhammad, A.A., Kashif, I., and Muhammad, J. "Evaluation of surface quality and mechanical properties of squeeze casted AA2026 aluminum alloy using response surface methodology", *The International Journal of Advanced Manufacturing Technology*, **103**, pp. 4041–4054 (2019). DOI: 10.1007/s00170-019-03836-6
11. Habib, S.S. "Study of the parameters in electrical discharge machining through response surface methodology approach", *Applied Mathematical Modelling*, **33**(12), pp. 4397–4407 (2019). DOI: 10.1016/j.apm.2009.03.021
12. Sarikaya, M. and Gullu, A. "Taguchi design and response surface methodology based analysis of machining parameters in CNC turning under MQL", *Journal of Cleaner Production*, **65**(15), pp. 604–616 (2014). DOI: 10.1016/j.jclepro.2013.08.040
13. Ghodsiyeh, D., Golshan, A., and Izman, S. "Multi-objective process optimization of wire electrical discharge machining based on response surface methodology", *Journal of the Brazilian Society of Mechanical Sciences and Engineering*, **36**, pp. 301–313 (2014). DOI: 10.1007/s40430-013-0079-x
14. Lmalghan, R., Karthik, M.C., and Arunkumar, S. "Machining parameters optimization of AA6061 using response surface methodology and particle swarm optimization", *International Journal of Precision Engineering and Manufacturing*, **19**, pp. 695–704 (2018). DOI: 10.1007/s12541-018-0083-2
15. Unune, D.R. and Mali, H.S. "Parametric modeling and optimization for abrasive mixed surface electro discharge diamond grinding of Inconel 718 using response surface methodology", *The International Journal of Advanced Manufacturing Technology*, **93**, pp. 3859–3872 (2017). DOI: 10.1007/s00170-017-0806-z
16. Lin, Y.C., Huang, J.Y., Wei, J.Y., et al. "Modeling and optimization of high-grade compacted graphite iron milling force and surface roughness via response surface methodology", *Australian Journal of Mechanical Engineering*, **16**(1), pp. 50–57 (2018). DOI: 10.1080/14484846.2017.1296531
17. Lu, X.H., Jia, Z.Y., Wang, H., et al. "The effect of cutting parameters on micro-hardness and the prediction of Vickers hardness based on a response surface methodology for micro-milling Inconel 718", *Measurement*, **140**, pp. 56–62 (2019). DOI: 10.1016/j.measurement.2019.03.037
18. Zhang, H., Zhang, J.S., Wang, Z., et al. "A new frame saw machine by diamond segmented blade for cutting granite", *Diamond and Related Materials*, **69**, pp. 40–48 (2016). DOI: 10.1016/j.diamond.2016.07.003
19. Zhang, H., Zhang, J.S., and Wang, S. "Comparison of wear performance of diamond tools in frame sawing with different trajectories", *Diamond and Related Materials*, **78**, pp. 178–185 (2019). DOI: 10.1016/j.ijrmhm.2018.09.012
20. Sun, Q., Zhang, J.S., Wang, Z., et al. "Segment wear characteristics of diamond frame saw when cutting different granite types", *Diamond and Related Materials*, **68**, pp. 143–151 (2016). DOI: 10.1016/j.diamond.2016.06.018
21. Sun, Q., Zhang, J.S., Wang, Z., et al. "Force and segment wear in various granites cutting by diamond frame saw", *Proceedings of the Institution of Mechanical Engineers, Part C: Journal of the Mechanical Engineering Sciences*, **203**(210), pp. 1989–1996 (2017). DOI: 10.1177/0954406217742937
22. Wang, F.Z., Liu, S.Y., Guo, Z.Y., et al. "Analysis of cutting forces and chip formation in milling of marble", *The International Journal of Advanced Manufacturing Technology*, **108**, pp. 2907–2916 (2020). DOI: 10.1007/s00170-020-05575-5
23. Ozfirat, P.M. "An integer programming approach for the three-dimensional cutting planning problem of marble processing industry", *The International Journal of Advanced Manufacturing Technology*, **59**, pp. 1057–1064 (2012). DOI: 10.1007/s00170-011-3574-1

24. Mehrannia, N., Kalantary, F., and Ganjian, N. "Experiment study on soil improvement with stone columns and granular blankets", *Journal of Central South University*, **25**, pp. 866–878 (2018). DOI: 10.1007/s11771-018-3790-z

25. Kalra, G. and Gupta, A.K. "Multi-response optimization of machining parameters in inconel 718 end milling process through RSM-MOGA", *The Scientific Temper*, **13**, pp. 01–13 (2022). DOI: 10.3390/machines12050335

26. Zhou, T. "Analysis of machined surface topography of AISI M2 in hard turning based on box-behnken design", *Proceedings of the Institution of Mechanical Engineers, Part B: Journal of Engineering Manufacture*, 095440542311572 (2023). DOI: 10.1177/09544054231157261

27. Choi, S., Lee, C., and Kim. D. "Experimental investigation for multiresponse optimization in rotary ultrasonic side milling of quartz", *The International Journal of Advanced Manufacturing Technology*, **122**, pp. 1583–1597 (2022). DOI: 10.1007/s00170-022-09993-5

28. Okokpujie, I.P., Tartibu, L.K., and Okokpujie. K. "Implementation of Box-Behnken design to study the factors interaction impacts and modelling of the surface roughness of AL 6063 alloys during turning operations", *International Journal on Interactive Design and Manufacturing (IJIDeM)* pp. 1-11 (2023). DOI:10.1007/S12008-023-01278-9/METRICS

29. Li, J., Zuo, W., and E, J.Q. "Multi-objective optimization of mini U-channel cold plate with SiO_2 nanofluid by RSM and NSGA-II", *Energy*, **242**, 123039 (2022). DOI: 10.1016/j.energy.2021.123039

30. Patel, K.A. and Brahmbhatt, P.K. "Response surface methodology based desirability approach for optimization of roller burnishing process parameter", *Journal of the Institution of Engineers (India): Series C*, **99**, pp. 729–736 (2018). DOI: 10.1007/s40032-017-0368-8

31. Hazir, E. and Ozcan. T. "Response surface methodology integrated with desirability function and genetic algorithm approach for the optimization of CNC machining parameters", *Arabian Journal for Science and Engineering*, **44**, pp. 2795–2809 (2019). DOI: 10.1007/s13369-018-3559-6

Biographies

Fangchen Yin received the BSE degree material processing from Shenyang University of Technology, China, and the MSE and PhD degrees in material processing from the Northeastern University, China, in 2013 and 2017, respectively. He is currently a Lecturer at the HuaQiao University. He has been involved in developing, designing, and commissioning of various areas of several robotic machining projects.

Hongyuan Zhang received the BSE degree mechanical manufacturing from HuaQiao University, China in 2021. He is currently working toward the PhD degree at the HuaQiao University. His research interests include stone processing with industrial robots, optimization of machining process parameters and robotic control theory.